

Kent Academic Repository

Full text document (pdf)

Citation for published version

Almoteriy, Mohammed and Sobhy, Mohammed and Batchelor, John C. (2018) Antenna Modeling Technique for Digital Communication Systems. In: Proceedings of the 15th International Conference on Synthesis, Modeling, Analysis and Simulation Methods and Applications to Circuit Design (SMACD). IEEE ISBN 978-1-5386-5152-0.

DOI

<https://doi.org/10.1109/SMACD.2018.8434852>

Link to record in KAR

<https://kar.kent.ac.uk/69369/>

Document Version

Author's Accepted Manuscript

Copyright & reuse

Content in the Kent Academic Repository is made available for research purposes. Unless otherwise stated all content is protected by copyright and in the absence of an open licence (eg Creative Commons), permissions for further reuse of content should be sought from the publisher, author or other copyright holder.

Versions of research

The version in the Kent Academic Repository may differ from the final published version.

Users are advised to check <http://kar.kent.ac.uk> for the status of the paper. **Users should always cite the published version of record.**

Enquiries

For any further enquiries regarding the licence status of this document, please contact:

researchsupport@kent.ac.uk

If you believe this document infringes copyright then please contact the KAR admin team with the take-down information provided at <http://kar.kent.ac.uk/contact.html>

Antenna Modeling Technique for Digital Communication Systems

Mohammed A. Almoteriy, Mohamed I. Sobhy, and John C. Batchelor

School of Engineering and Digital Arts, University of Kent, Canterbury, United Kingdom
{Maa74, M.I.Sobhy, J.C.Batchelor}@kent.ac.uk

Abstract— This paper demonstrates the characterization and modeling of an antenna to predict its effect when used in a digital communication system. The technique was applied to a commercial dual-band antenna. An equivalent circuit model was derived to characterize the antenna behavior in the frequency domain. A time domain system model was also derived to enable the estimation of the antenna effects in a digital system. The results show that the antenna caused symbol scattering and contributed to the error vector magnitude.

Keywords—transfer function, equivalent circuit, antenna phase, antenna effects, impulse response, digital communication system.

I. INTRODUCTION

Antenna engineers commonly design antennas for a low input reflection coefficient (S_{11}) using simulations and measurements. They then obtain the gain and radiation patterns at certain frequencies. These parameters are insufficient to completely characterize the antenna as a two-port network. This procedure also does not provide essential antenna parameters such as the S_{11} phase and the complex transfer parameter, S_{21} . Those parameters are important in digital communication systems (DCSs), which are simulated and studied in the time domain. The aim of the current study is to derive a time domain system model from the antenna frequency domain measurement. This technique is applied to model and characterize antennas to be included in DCS software. This technique enables designers to predict the effects of an antenna on the modulated signal in a DCS and to estimate the symbol scattering. The error vector magnitude (EVM) and bit error rate (BER) are commonly accepted metrics used in characterizing symbol scattering and in examining system performance. These steps also help to identify sophisticated antenna structures that will minimize the effect of the antenna in the DCS.

Two-port equivalent circuit models (ECMs) can be derived to obtain the S_{21} . The models characterize the antenna behavior and predict the total radiated power [1]. The derivation of an ECM for an antenna is derived by defining the topology based on antenna structure and using only complex S_{11} to obtain the circuit element values [2]. The radiation resistance is identified in the second port and the radiated power is the power dissipated in that resistance. Antennas are also categorized into minimum and non-minimum phase [3]–[5]. Minimum-phase antennas have only a single path for the energy transferred through the antenna's equivalent circuit [6]. Non-minimum phase antennas, in contrast, have several paths for energy transfer.

Alongside the current exponential growth in wireless communications, the application of antennas in wireless systems

has also increased significantly. Understanding antenna effects in DCSs has become an important part of achieving good system performance [2], [7]. Designers aim to have wideband antennas and non-dispersive signals. BER can be caused from fading channels, non-linearity in the radio frequency (RF) components, added noise in the channel and from properties of the antenna system. These effects increase the symbol scattering of the systems and result in performance degradation.

In this paper, the commercial dual-band antenna shown in Fig. 1 was characterized and modeled. An ECM was derived for the antenna to obtain the total radiated power and to characterize the antenna behavior. The full set of S-parameters were measured in an anechoic chamber between two identical antennas in order to compare the resulting S_{21} in amplitude and phase with the values obtained from the ECM. A Finite Impulse Response (FIR) model was derived for each S-parameter to represent a time domain system model for the antenna. The antenna system model was then simulated on a DCS with 16-QAM modulation to predict the antenna effects on the system in the two bands at two different carrier frequencies.

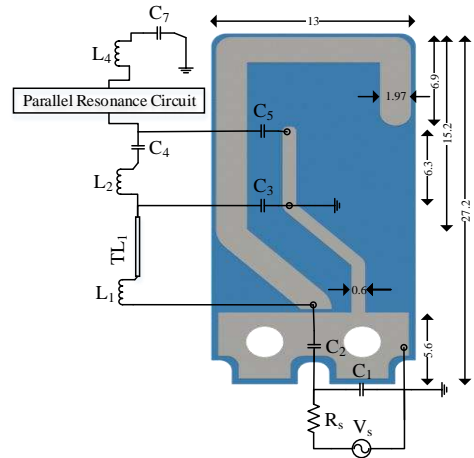


Fig. 1. Commercial dual-band antenna structure and ECM topology (all dimensions in mm).

II. EQUIVALENT CIRCUIT MODEL (ECM)

A commercial dual-band antenna was printed on an FR-4 dielectric and had planar features. The first step was to define the topology, as mapped to the antenna structure shown in Fig. 1. The antenna is represented by the transmission line TL1 and inductors L1, L2, and L4, whereas capacitors represent the coupling to the ground. The ECM was simulated and optimized to match the complex S_{11} using Advanced Design System®

(ADS) software. The ECM for the antenna was then derived, as illustrated in Fig. 2, and the radiation resistance of the antenna was found to be at 63 Ω . The S1P block shown in Fig. 2 contains the S_{11} data measurement result obtained using a network analyzer. This block was used to optimize the circuit to match the S_{11} measurement by using an iterative optimization process in the ADS software. The ECM showed a single path for transferring energy through the equivalent circuit, which confirmed that the antenna is a minimum phase antenna [6]. The S_{11} from the ECM was then compared with the measurement. Both values were found to match, as shown in Fig. 3. The antenna had two radiating bands at the two resonance frequencies 2 GHz and 6 GHz.

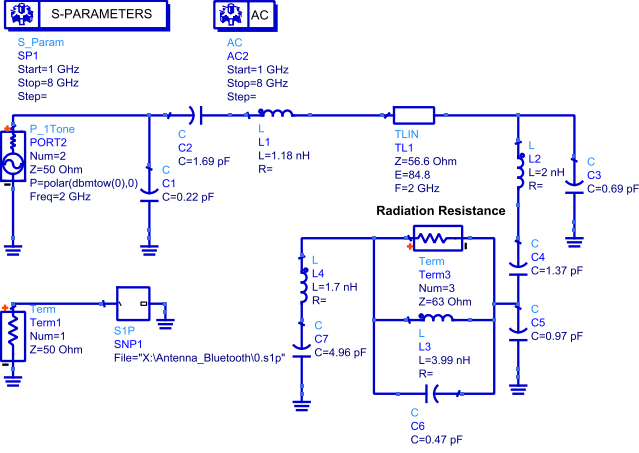


Fig. 2. ECM for the commercial dual-band antenna.

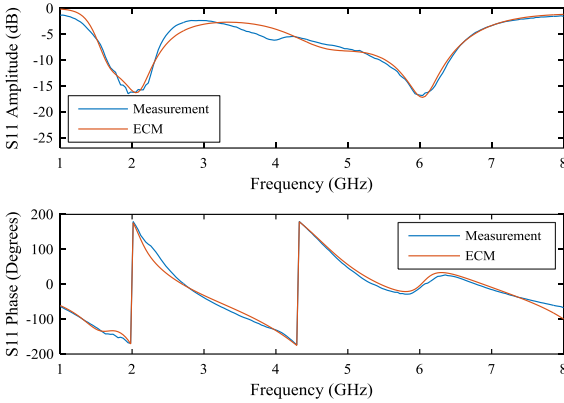


Fig. 3. Comparison of S_{11} from measurements and from ECM.

S_{21} measurements were then conducted in an anechoic chamber between two identical antennas on their principal axis, 70 cm apart, using a network analyzer. The amplitude and phase of S_{21} for each antenna were obtained after de-embedding the free-space channel, taking the square root of the amplitude, and dividing the phase by two. Assuming the antenna is lossless and that all observed power is radiated. The S_{21} which represents the total radiated power of each antenna can be calculated from S_{11} by [8]:

$$|S_{21}| = \sqrt{1 - |S_{11}|^2} \quad (1)$$

The S_{21} from the ECM matched that computed from S_{11} using (1), as shown in Fig. 4; this response represents the power ratio of the total radiated power. The measured S_{21} of the antenna after de-embedding the free-space channel is also shown in Fig. 4, which represents the radiated power from the antenna on the antenna's principal axis. The remaining power was radiated on the sidelobes.

As shown in Fig. 5, the phase of S_{21} obtained from the ECM matched that obtained from the measurement, and both were found to be linear in phase. This situation indicates that only minimum-phase and linear-phase components were found in the S_{21} phase [1], which in turn confirms that the antenna is a minimum phase and that its behavior had a frequency-invariant radiation pattern [9].

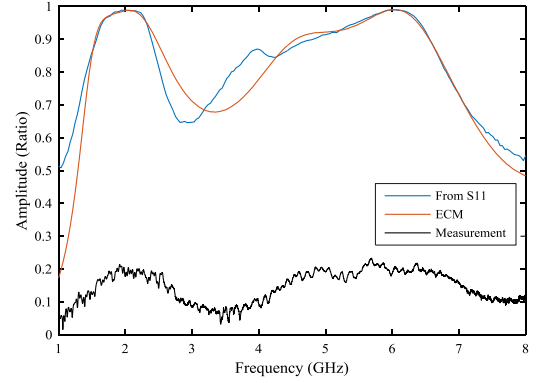


Fig. 4. Amplitude of S_{21} from the ECM, from S_{11} , and from measurement.

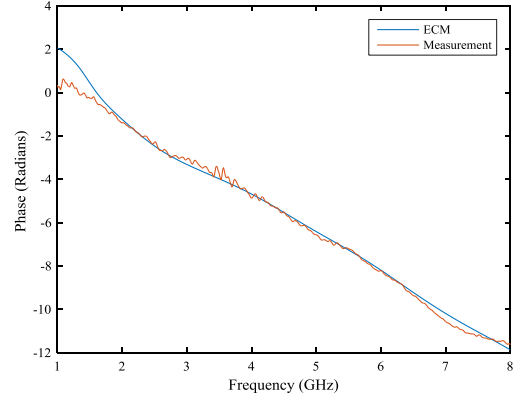


Fig. 5. S_{21} phase from the measurement and the ECM.

III. ANTENNA SYSTEM MODEL

Modeling an antenna as a system is a technique for analyzing the effects of an antenna in DCS software. Modeling is developed to determine the computability of the antenna in a DCS simulation. S-parameters can be measured between transmitting and receiving antennas [4]-[6]. The measurement of a full set of S-parameters enables the designer to predict the correct frequency response in the direction of communication. The system model is derived by realizing the complete S-parameters from the measurement between transmitting and receiving antennas. This derivation also helps designers to model accurate system models with precise S_{11} , S_{21} , S_{12} , and S_{22} measurements. The impulse response in the time domain was

obtained by applying the inverse fast Fourier transform (IFFT) to each complex S-parameter. When using two identical antennas in the measurement, the S_{11} and S_{22} are the same, as are S_{12} and S_{21} . From the full set of S-parameters measured in the anechoic chamber, FIR models were then derived for each S-parameter with a 4,001-order to develop four models for the S-parameters.

The validity of the antenna system model derived from the FIR models was then verified. The impulse response of the FIR model was compared with the impulse response of each S-parameter obtained from the frequency response measurement, and the values were found to match. The impulse response of the S_{21} measurement and the antenna S_{21} FIR model are shown in Figs. 6a and b, respectively; both values are shown to be similar. The impulse response of the antenna S_{21} had many components due to multiple reflection in the antenna system.

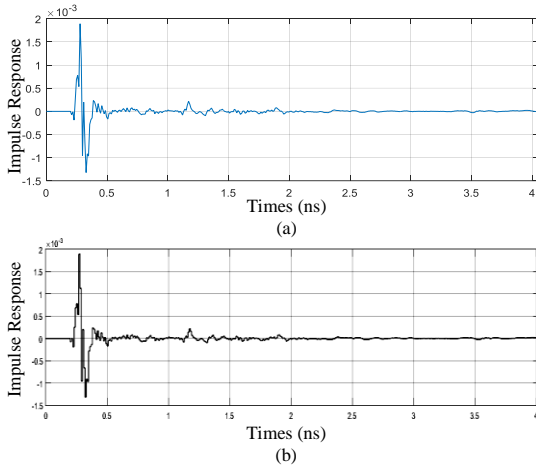


Fig. 6. Impulse response of (a) antenna S_{21} measurement and (b) the antenna S_{21} FIR model.

The complete system model with four FIR models derived for the full set of the S-parameters was then developed, as shown in Fig. 7. The chirp signal in the input of the system is a frequency swept source, to predict the frequency response of the antenna system. Fig. 8a shows the frequency response of the system model. This is compared to the S_{21} measurement shown in Fig. 8b, which contained the response of the two identical antennas with a 70 cm path-length free-space channel. Antenna measurements were then modeled as a two-port network system to evaluate the performance of the antenna in a system simulation that could then be used directly in DCS software.

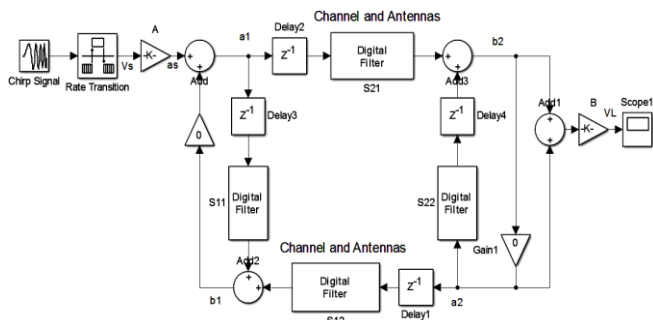


Fig. 7. Complete antenna system model with four FIR models.

The system model shown in Fig. 7 was then used to study the antenna effect on transmitted signals and to calculate the EVM as well as the resulting BER of a DCS [2]. This technique allows designers to assess the system performance resulting from the antenna effects, such as symbol scattering that leads to the degradation of system performance. Fig. 9 shows the steps involved in predicting the effects of an antenna in a DCS, starting from the frequency response antenna measurement.

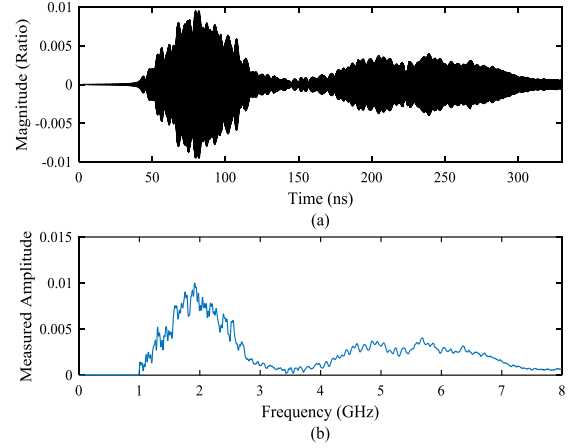


Fig. 8. Frequency response of the (a) antenna system and (b) S_{21} measurement.

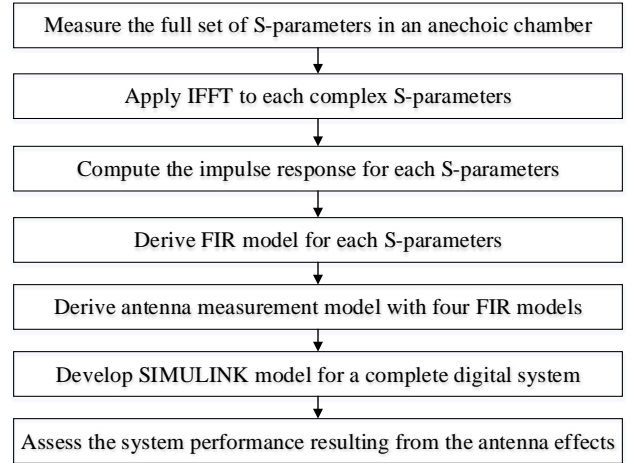


Fig. 9. Flow chart to predict antenna effects in a DCS.

IV. ANTENNA SIMULATION IN A DCS

A complete DCS was modeled in SIMULINK to simulate the antenna model as illustrated in Fig. 10. This model was derived to predict the effects of the antenna and to obtain the EVM and BER for characterizing the symbol scattering. The DCS consists of a data generator that is then modulated by 16-QAM. An up-converter was used to send the data with a carrier frequency to convert the transmission data from baseband to passband followed by the antenna system model. FIR models represented the full set of S-parameters of the antenna measurement from the two identical antennas with the free-space channel. The signal was then passed through the down-converter to convert the signal back to the baseband-modulated signal. This step was performed without adding any noise so that the antenna effect on the DCS could be predicted.

In the DCS simulation, the antenna was examined at two different carrier frequencies with 10^6 symbols. The effects of the antenna on the modulated signal were then investigated. The antenna effects on the DCS performance are shown in the constellation diagrams in Figs. 11a and 11b for the two carrier frequencies of 2 GHz and 6 GHz, respectively. The output constellation diagrams show that the antenna caused symbol scattering with varying EVMs. The EVM was 11.95% and 6.16% in the carrier frequency 2 GHz and 6 GHz, respectively. The BER was zero because the receiver was able to recover the symbols in spite of scatter. This scattering occurred because the antenna impulse response produced other components due to multiple reflection in the antenna, which caused the symbol scattering shown in the constellation diagrams. The comparisons between the two carrier frequencies in the constellation diagrams and the EVM showed that the symbol scattering at 2 GHz was more severe than at 6 GHz, which estimated the antenna effects on the modulated symbol in the two bands. This technique is also useful to predict the performance of the system in each band in multiband systems.

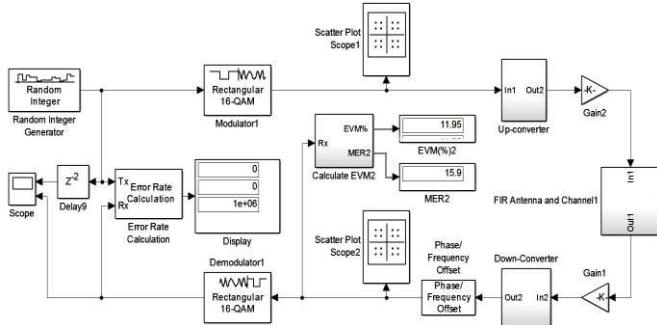


Fig. 10. Antennas with free-space channel in a DCS.

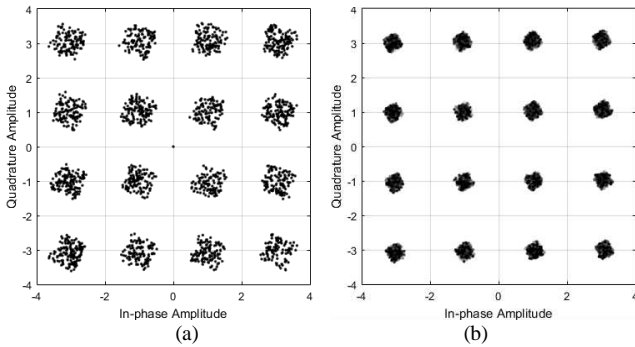


Fig. 11. Output constellation diagrams after antenna system model at carrier frequency (a) 2 GHz and (b) 6 GHz.

The effects on a DCS depends on the antenna types employed. An antenna impulse response is an important parameter, especially if the antenna produces additional components due to multiple reflection in the antenna itself, which will increase the effects on a DCS's performance. This technique allows for simulating an antenna in a DCS and enables designers to predict the effects of an antenna in a DCS. Doing so also allows designers to modify and redesign antennas for robust digital system performance. Once antenna models are derived,

the different antennas and channels can be used for different applications. This is the case when a base station is transmitting and many users are receiving signals.

V. CONCLUSION

This paper has described a technique to characterize and model an antenna to be included in DCS simulation; it also reported on the effect of the antenna on wireless links and DCSs. The ECM for a commercial dual-band antenna was derived, and the S_{21} was obtained in both amplitude and phase. The total radiated power was computed, and the antenna behavior was characterized. The FIR models were derived for all S-parameters from the frequency response antenna measurement to be able to include the antenna in a DCS simulation. The impulse response of the antenna showed additional components due to multiple reflection in the antenna. The effects from the antenna only were predicted in a DCS, and the EVM and BER were calculated to characterize the symbol scattering. The results showed that the antenna caused symbol scattering and that the EVM had increased at the receiver for both bands at the two carrier frequencies. The antenna effects at 6 GHz were shown to have less of an effect compared to the effects at 2 GHz. This scattering, and the change in EVM, were caused by the antenna design. These effects reduced the order of the modulation scheme and the data-transmission rates. This technique enables designers to predict the performance of a multiband system in each band. This technique will allow engineers to integrate antennas with fading channels in DCS simulations for different applications for future work.

REFERENCES

- [1] M. Almotery, M. Sobhy and J. Batchelor, "Antenna characterisation and channel effects on digital systems," Loughborough Antennas & Propagation Conference, 2017, in press.
- [2] M. I. Sobhy, B. Sanz-Izquierdo and J. C. Batchelor, "System and Circuit Models for Microwave Antennas," IEEE Transactions on Microwave Theory and Techniques, vol. 55, (4), pp. 729-735, 2007.
- [3] J. S. McLean, R. Sutton and H. Foltz, "Minimum phase / all-pass decomposition of LPDA transfer functions," IEEE International Conference on Ultra-Wideband, 2009.
- [4] H. Foltz et al, "UWB antenna transfer functions using minimum phase functions," IEEE Antennas and Propagation Society International Symposium, 2007.
- [5] J. S. McLean, H. Foltz and R. Sutton, "Differential time delay patterns for UWB antennas," in 2008 IEEE International Conference on Ultra-Wideband, 2008.
- [6] J. S. McLean, H. Foltz and R. Sutton, "Directional dependence of the minimum phase property of antenna transfer functions," in Antennas & Propagation Conference, 2009. LAPC 2009. Loughborough, 2009.
- [7] T. Prakoso et al, "Antenna representation in two-port network scattering parameter," Microwave Opt Technol Lett, vol. 53, (6), pp. 1404-1409, 2011.
- [8] D. M. Pozar, "The scattering matrix in microwave network analyzer," in Microwave Engineering, 4th ed. Anonymous New Jersey: John Wiley & Sons, 2012, pp. 177-183.
- [9] D. Panaitopol et al, "Impact of the design of an UWB antenna on the maximum achievable rate of the communication in presence of multi user interferences," Asia-Pacific Microwave Conference, 2008.